Available online at www.sciencedirect.com
ScienceDirect
Polymer 48 (2007) 2745–2754
polymer
www.elsevier.com/locate/polymer

Effect of hydrogen bonding on the crystallization behavior of poly(3-hydroxybutyrate-*co*-3-hydroxyhexanoate)/silica hybrid composites

Jung Seop Lim [a], Isao Noda [b], Seung Soon Im [a,*]

[a] *Department of Fiber and Polymer Engineering, College of Engineering, Hanyang University, 17, Haengdang-dong, Seongdong-gu, Seoul 133-791, Republic of Korea*
[b] *The Procter & Gamble Company, West Chester, OH 45069, USA*

Received 27 November 2006; received in revised form 9 March 2007; accepted 9 March 2007
Available online 15 March 2007

Abstract

Biodegradable poly(3-hydroxybutyrate-*co*-3-hydroxyhexanoate) (PHB-HHx)/hydrophobically modified silica hybrid composites were prepared using simple melt compounding and the effect of hydrogen bonding on their crystallization behavior was observed. The intermolecular hydrogen bonding between PHB-HHx and silica increased gradually with the increase of silica content of the hybrid composites. However, the extent of intermolecular hydrogen bonding was not directly proportional to the silica content. Although, the crystallization rates of the PHB-HHx/silica hybrids decreased as the strength of intermolecular hydrogen bonding increased, the constant value of the Avrami exponent indicates that the presence of silica does not alter the nucleation mechanism or the geometry of the crystal growth of the PHB-HHx hybrids. The calculated crystallization activation energy increased with the addition of silica, suggesting that silica retards the overall crystallization rate of the PHB-HHx hybrid composites as a result of the existence of intermolecular hydrogen bonding. The relationship between the extent of intermolecular hydrogen bond and crystallization rate is described by the empirical second-order equation.

Keywords: Poly(3-hydroxybutyrate-*co*-3-hydroxyhexanoate) (PHB-HHx); Silica; Hydrogen bonding

1. Introduction

As the interest in industrial application of biodegradable polymers is growing, biodegradable polymer/inorganic hybrid composites, made by adding a small amount of inorganic material within a matrix of polymer, have attracted much attention. Such hybrid composites sometimes exhibit substantially improved thermal, mechanical, and physical properties in comparison to the corresponding neat polymer [1–3]. They can combine the favored properties of the inorganic material (e.g., increased strength and modulus, high thermal stability and better gas barrier property) and the organic polymer matrix (e.g., flexibility, low density and processability).

Poly(3-hydroxybutyrate-*co*-3-hydroxyhexanoate) (PHB-HHx) is a relatively new member of the polyhydroxyalkanoate (PHA) family, which has gained popularity as a useful biodegradable polymer due to superior thermoplasticity, excellent biocompatibility, and biodegradability [4,5]. Nevertheless, in certain practical applications, PHB-HHx suffers from limitations, such as its thermal stability and insufficient mechanical stiffness. Hybrids made of PHB-HHx and inorganic materials may circumvent these limitations of the PHB-HHx and to expand its applications.

Fumed silica is a useful reinforcing agent for polymer/inorganic hybrids. However, this inorganic material is strongly hydrophilic due to the numerous silanol groups on its surface and exhibits a very high surface energy, which in turn leads to its tendency to aggregate in the composites. Thus, in order to reduce the surface energy of silica and prevent the subsequent aggregation, fumed silica may be hydrophobically modified. Such hydrophobically modified silica particles are more readily dispersed in the polymer matrix and produced improved organic/inorganic hybrid composites [6,7].

* Corresponding author. Tel.: +82 2 2220 0495; fax: +82 2 2297 5859.
E-mail address: imss007@hanyang.ac.kr (S.S. Im).

0032-3861/$ - see front matter © 2007 Elsevier Ltd. All rights reserved.
doi:10.1016/j.polymer.2007.03.034

With organic/inorganic hybrids, specific interactions, such as hydrogen bonding between the organic polymer matrix and the inorganic phase are often very important. Such interactions can alter the polymer crystallization rate, crystallinity, morphology, and microstructure [8–10]. Most importantly, the relationship between hydrogen bonding and the crystallization rate needs to be carefully examined, because this effect can be a major factor which affects the physical properties and processing conditions of final product, such as spinning, extrusion, compression and injection molding.

Until now, studies of biodegradable polymer/inorganic hybrid composites have traditionally focused mainly on the dispersibility of the inorganic materials within the polymer matrix and the resulting physical properties. Relatively little has been reported on the influence of hydrogen bonding on the crystallization behavior. Further, few investigations have examined PHB-HHx/inorganic hybrids.

In this study, PHB-HHx/hydrophobically modified fumed silica hybrid composites were prepared by using simple melt blending and the effects of hydrogen bonding on their crystallization behavior were ascertained. The hybrid composites not only showed great potential for advanced material applications, but also helped to clarify how addition of the inorganic component modifies the crystallization mechanisms.

2. Experimental

2.1. Materials and sample preparation

The bacterial polyester, poly(3-hydroxybutyrate-*co*-3-hydroxyhexanoate) (PHB-HHx), was supplied by the Procter & Gamble Company (Cincinnati, USA). It contained the 3-hydroxy hexanoate content of about 12 mol% and the weight average molecular weight (M_w) of 1,388,000 with the polydispersity of about 2.0. Fumed silica, Aerosil R300 and Aerosil R812 (Degussa Chemical, Düsseldorf, Germany), were used to prepare the hybrid composites. Aerosil R300 has pronounced hydrophilic properties, while Aerosil R812 is a hydrophobically modified fumed silica produced by treatment with hexamethyl disilane. It has the specific surface area of $260 \pm 30\ m^2\ g^{-1}$, average particle size of 7 nm, and degree of hydrophobicity of about 42%.

PHB-HHx/silica hybrid composites were prepared by the direct melt compounding by using a twin roll counter-rotating mixer (Thermo Haake, Paramus, NJ, USA). The barrel temperature was set to be 165 °C and the screw speed was 100 rpm. The total mixing time was 2 min. Before melt compounding in a one-step process, the PHB-HHx was ground and mixed with silica. After melt compounding, films were prepared using a hot press at 165 °C with the holding pressure of 6000 psi and the holding time of 5 min. The hybrids consisted of PHB-HHx/hydrophilic fumed silica and PHB-HHx/hydrophobically modified fumed silica ratios of 100/0, 99/1, 97/3, and 95/5 by weight. The prepared films were quenched in cold water.

2.2. Measurement

Fourier transform infrared (FT-IR) spectra were obtained at room temperatures on an IFS 88-IR spectrometer (Bruker AXS GmbH, Karlsruhe, Germany). The scanned wavenumber range was 4000–400 cm^{-1}. All spectra were recorded at a resolution of 4 cm^{-1}, and 16 scans were averaged for each sample. Scanning electron microscopy (SEM) of the PHB-HHx/silica hybrid films was undertaken after fracturing the films under liquid nitrogen and drying at room temperature. The samples were gold coated by ion sputtering and examined by using field emission (FE) SEM (JSM-6700F, JEOL, Tokyo, Japan). The thermal properties of 6 mg sample of each PHB-HHx/silica hybrid composite in a sealed aluminum sample pan were analyzed using a Perkin–Elmer DSC7. All the samples were heated at 5 °C min^{-1} from −40 to 180 °C and then maintained at 180 °C for 3 min, before cooling to −40 °C at 1, 2, 3, or 5 °C min^{-1}. Subsequently, the samples were reheated at 5 °C min^{-1}. The isothermal crystallization of the PHB-HHx/silica hybrids was analyzed by heating each sample from −10 to 200 °C at 40 °C min^{-1} and then maintaining it at 200 °C for 5 min to erase the previous thermal history. The samples were then quenched to their crystallization temperatures at 150 °C min^{-1} and the isothermal crystallization exotherm was recorded for 60 min. The spherulitic morphology of the hybrid samples was investigated by using a Nikon polarized light microscope (Nikon, Tokyo, Japan). Each sample was melted on a hot stage at 190 °C for 1 min and then quickly transferred to a Mettler-Toledo FP82HT hot stage and equilibrated at the desired crystallization temperature (Mettler-Toledo, Greifensee, Switzerland). Crystallization occurred over 60 min and the spherulitic morphology of the samples was examined when crystallization was complete.

3. Results and discussion

3.1. Intermolecular hydrogen bonding

Fig. 1 shows the IR spectra in the hydroxyl group regions of hydrophilic and hydrophobic silica. The hydrophilic silica shows a broad band centered at 3435 cm^{-1}, reflecting the intramolecular hydrogen-bonded silanol hydroxyl groups [11]. In hydrophobic silica, the hydroxyl band shifts to a higher wavenumbers and its peak occurs near 3441 cm^{-1} with a reduced intensity. These results indicate that the intramolecular hydrogen bonding in hydrophobic silica is weaker than that of the hydrophilic silica as a result of a relatively small amount of hydroxyl groups [12].

Fig. 2(a) and (b) shows the IR spectra in the 1800–1680 cm^{-1} carbonyl region of the PHB-HHx/hydrophobically modified silica and PHB-HHx/hydrophilic silica hybrid composites, respectively. The amorphous carbonyl peak of pure PHB-HHx occurs at about 1730 cm^{-1}. As the silica content of the hybrids increases, the carbonyl peak shifts to lower wavenumbers, suggesting that the intermolecular hydrogen bonding in the PHB-HHx/silica hybrids increases with the

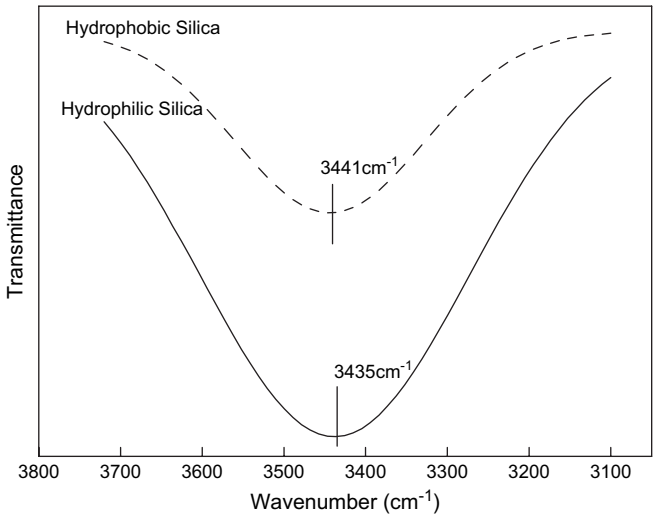

Fig. 1. IR spectra in the hydroxyl group region of hydrophilic silica and hydrophobic silica.

added silica content. However, compared with the PHB-HHx/hydrophilic silica hybrids, the carbonyl peaks of the PHB-HHx/hydrophobically modified silica hybrids occur at lower wavenumbers. The maximum extent of the carbonyl peak shift is about 3 cm^{-1} for the PHB-HHx/hydrophobic silica (5 wt%) composites for which the carbonyl peak lies near 1727 cm^{-1}. On the other hand, carbonyl peak of the PHB-HHx/hydrophilic silica (5 wt%) moves down only by about 1 cm^{-1}, so that this peak is located at about 1729 cm^{-1}. These results demonstrate that hydrophobically modified silica, with a relatively small amount of hydroxyl groups, contains weaker intramolecular hydrogen bonding than hydrophilic silica. Hence, intermolecular hydrogen bonds may be more easily formed with the carbonyl group of the PHB-HHx.

Fig. 3 shows the IR spectra in the hydroxyl group region of the PHB-HHx/hydrophobically modified silica hybrids. On forming hybrids with silica, the OH band appears at 3418 cm^{-1} for PHB-HHx/silica (1 wt%) hybrids and gradually shifts to 3407 and 3401 cm^{-1}, respectively, as the silica content increases from 3 to 5 wt%. This result may be attributed to the fact that with a higher silica content, more silica hydroxyl groups can take part in the intermolecular hydrogen bonding with the carbonyl groups of PHB-HHx.

To better understand the intermolecular hydrogen bonding interaction between the PHB-HHx and hydrophobically modified silica in the hybrid composites, the vibrational force constant was calculated as in Ref. [12] and displayed in Table 1. If intermolecular hydrogen bonding occurs between a hydroxyl group of silica and the carbonyl group of PHB-HHx, the hydroxyl bond energy of silica is reduced owing to the interaction between the H atom in the hydroxyl group and the O atom of the carbonyl group. Consequently, the force constant of the hydroxyl group will exhibit lower values. As seen in Table 1, the force constant of the PHB-HHx/hydrophobically modified silica decreases gradually as the silica content increases, confirming that the intermolecular hydrogen bond between the hydroxyl group of silica and the carbonyl groups

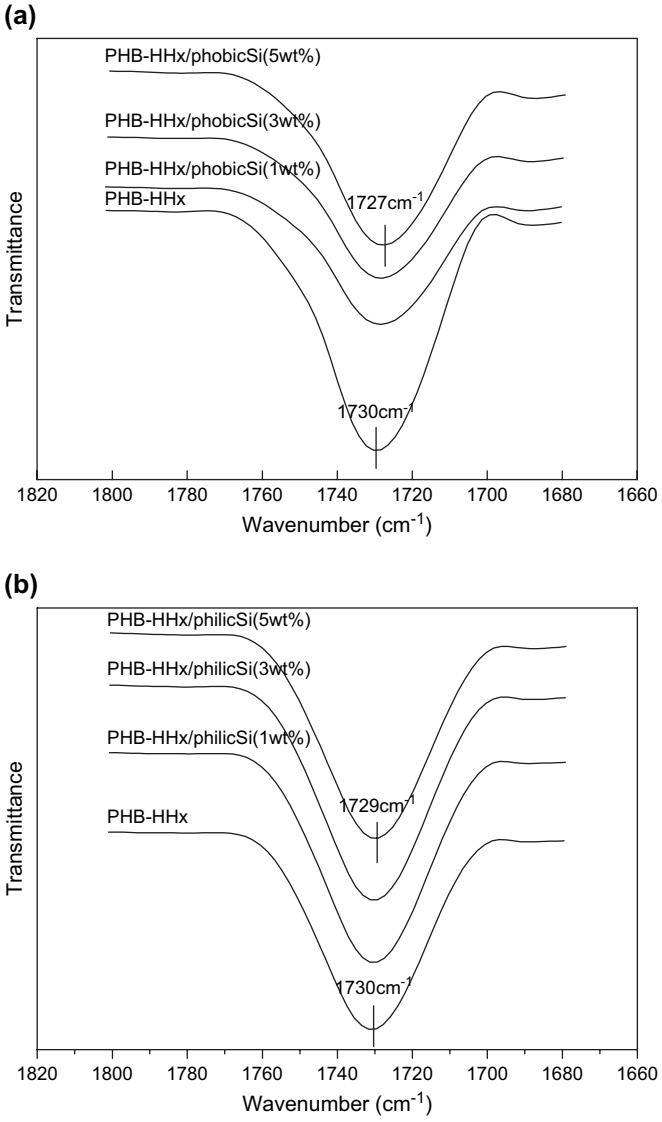

Fig. 2. IR spectra of the carbonyl group region of PHB-HHx/silica hybrid composites: (a) PHB-HHx/hydrophobically modified silica and (b) PHB-HHx/hydrophilic silica.

of PHB-HHx is enhanced in the hybrid composites as the silica content increases.

3.2. Quantitative analysis of the intermolecular hydrogen bond fraction

Fig. 4 shows the IR spectra in the 3100–2700 cm^{-1} region of the PHB-HHx/hydrophobically modified silica hybrid composites. The groups of bands in the 2980 and 2880 cm^{-1} region can be assigned, respectively, to the CH_3 asymmetric and symmetric stretching peaks, where pure PHB-HHx has a relatively larger CH_3 asymmetric stretch peak than any of the PHB-HHx/hydrophobically modified silica hybrid composites do. Generally, CH_3 asymmetric stretch peak appears when a bonding energy of three CH stretches is imbalanced. It is reported that an inter- or intramolecular hydrogen bond between O atom of the C═O group and the H atom of one

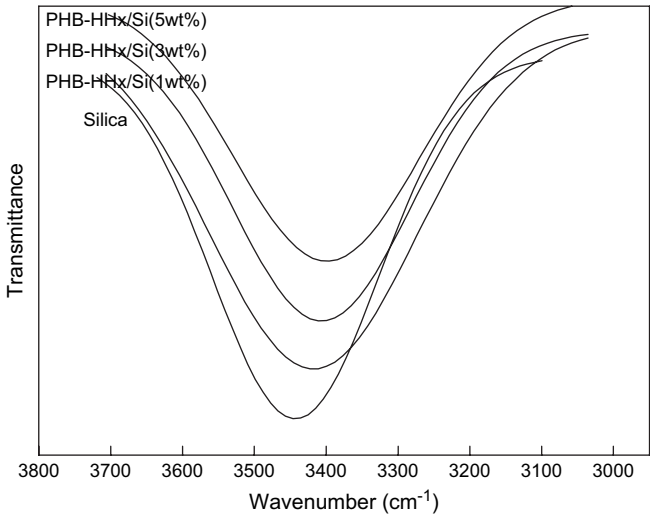

Fig. 3. IR spectra of the hydroxyl group region of the PHB-HHx/hydrophobically modified silica hybrid composites.

Table 1
Wavenumbers and force constants of the hydroxyl group for the PHB-HHx/hydrophobically modified silica hybrid composites

Sample	The wavenumber of hydroxyl peak (cm^{-1})	The force constant (dyn/cm)
Hydrophobically modified silica	3441	6.56×10^5
PHB-HHx/Si (1 wt%)	3418	6.47×10^5
PHB-HHx/Si (3 wt%)	3407	6.43×10^5
PHB-HHx/Si (5 wt%)	3401	6.41×10^5

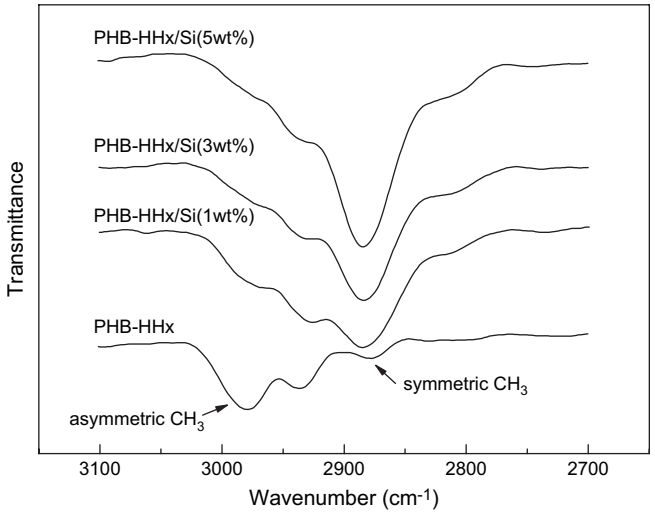

Fig. 4. IR spectra in the 3100–2700 cm^{-1} region of the PHB-HHx/hydrophobically modified silica hybrid composites.

of the C–H bonds of the CH_3 group in the PHB-HHx [13]. Based on this, relatively larger CH_3 asymmetric stretch peak of the PHB-HHx can be explained that the bonding energy in three C–H bonds is not balanced due to hydrogen bond within PHB-HHx.

With the increase of silica content, it can be found that the CH_3 asymmetric stretch peak is gradually decreased. Meanwhile, the intensity of CH_3 symmetric stretch peak becomes more intense, indicating that the bonding energy of three CH stretches within CH_3 groups is same. This can be attributed that the addition of silica breaks down the inter- or intramolecular hydrogen bond between the carbonyl group and the methyl group within the PHB-HHx, leading to the balance of bonding energy in three C–H stretches. Accordingly, more free carbonyl groups of the PHB-HHx contribute to the intermolecular hydrogen bonding with the hydroxyl groups of the silica in the hybrids, resulting in the shift of carbonyl group in the PHB-HHx as seen Fig. 2. The likely mechanism is shown schematically in Fig. 5.

The fraction of intermolecular hydrogen bonds formed between carbonyl groups in the PHB-HHx and the hydroxyl groups of silica was estimated from the ratio between the relative peak intensities of the symmetric and asymmetric CH_3 stretching bands. Fig. 6 shows the variation in the intermolecular hydrogen bond fraction as a function of the silica content in the PHB-HHx/hydrophobically modified silica hybrid composites. The maximum value occurs at 5 wt% silica content,

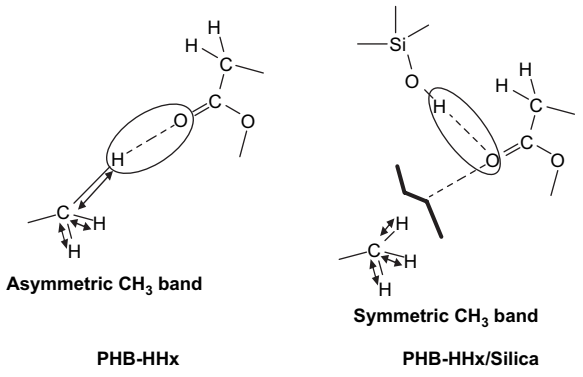

Fig. 5. Schematic representation of the mechanism of intermolecular hydrogen bonding in the PHB-HHx/hydrophobically modified silica hybrid composites.

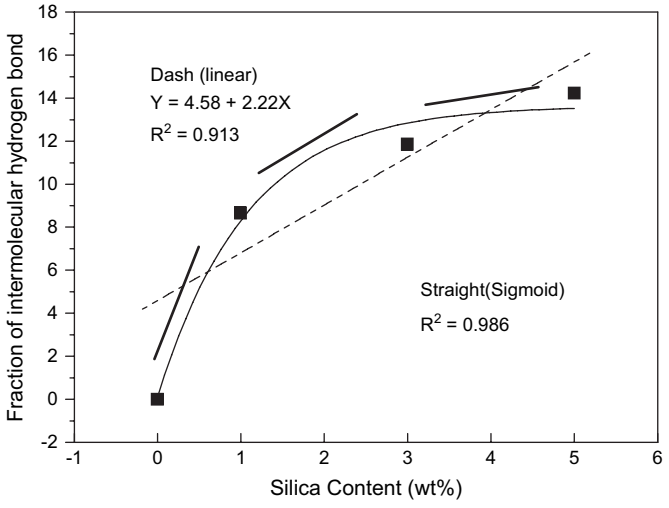

Fig. 6. The variation in the intermolecular hydrogen bond fraction as a function of the silica content in the PHB-HHx/hydrophobically modified silica hybrid composites.

indicating that this silica composition is the point where the intermolecular hydrogen bond is the strongest.

Further, the fraction of intermolecular hydrogen bonds increases sharply as the silica content increases from 0 to 1 wt%, but increases only moderately at higher silica contents. Both linear and sigmoid fits were applied to the PHB-HHx/hydrophobic silica hybrid data in an attempt to establish the correlation between the extent of intermolecular hydrogen bonding and silica contents. As shown in Fig. 6, the sigmoid fit proves better than the linear with a reliability of 0.986 *vs.* 0.913, respectively, suggesting that the silica content is not directly proportional to the extent of intermolecular hydrogen bonding.

In general, molecules containing hydroxyl groups, such as silica, phenol, and 2-propanol, have intramolecular hydrogen bonds between hydroxyl groups, which may become an important factor determining the extent of intermolecular hydrogen bonding in polymer composites [14]. For example, when a substance possesses a large amount of intramolecular hydrogen bonding within itself, then the presence of this intramolecular hydrogen bond will limit the extent of hydrogen moieties that can associate with the intermolecular hydrogen bond. Consequently, this result can be explained as the following. At a relatively low silica content, most of the hydroxyl groups participate in creating the intermolecular hydrogen bonding with the carbonyl groups of PHB-HHx. By contrast, at higher silica contents, additional amount of hydroxyl groups not only forms intermolecular hydrogen bond with the carbonyl groups of PHB-HHx but also contributes to the intramolecular hydrogen bond. Therefore, the relative increase in intermolecular hydrogen bonding at a high silica content may be lower than that observed by the addition of only a small amount silica in the PHB-HHx matrix. Fig. 7 shows this mechanism schematically. This model concurs with the work of Li and Brisson, who showed that in poly(methyl methacrylate)/poly(vinyl phenol) (PMMA/PVPh) blends, both intra- and intermolecular hydrogen bonds exist at high PVPh compositions, but only intermolecular hydrogen bonding occurs at low PVPh compositions [15].

Fig. 8(a)–(c) shows the SEM micrographs of the PHB-HHx/hydrophobically modified silica hybrid composites. It is well known that silica readily aggregates with each other due to intramolecular hydrogen bonding [16]. The hybrid composites in Fig. 8 show various sizes of aggregates for a given silica content. For a silica content of 1 wt%, the silica particles disperse effectively in the PHB-HHx matrix and exhibit only aggregates with particle size of less than 100 nm. However, at a silica content of 5 wt%, the number of large aggregates increases markedly. Some of the aggregates even exceed the size of 250 nm. This result supports the view that the higher the silica content is, the larger the silica aggregates becomes due to the strong intramolecular hydrogen bonding that takes place between the hydroxyl groups in silica.

3.3. Non-isothermal crystallization behavior

Fig. 9(a) and (b), respectively, shows the DSC cooling curves for the PHB-HHx/hydrophobically modified silica hybrid obtained at cooling rates of 1 and 3 °C min^{-1}. All the samples show only one exothermic peak, pointing to the crystallization of a single phase. As the cooling rate increases, the

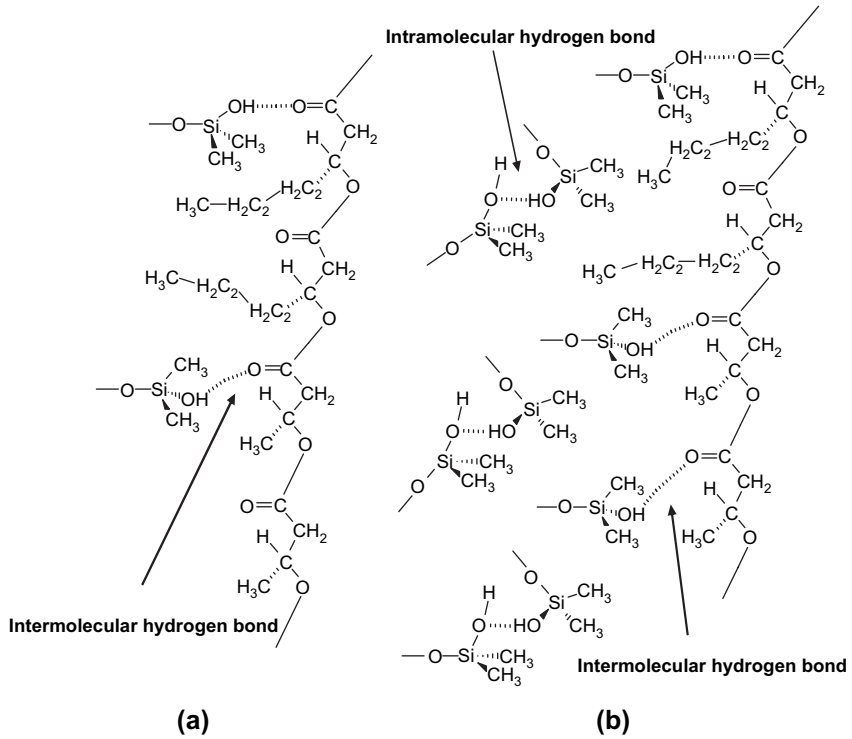

Fig. 7. Schematic representation of the hydrogen bonding interaction in the PHB-HHx/hydrophobically modified silica hybrids: (a) low silica composition, exhibiting intermolecular hydrogen bond and (b) high silica composition, showing intra- and intermolecular hydrogen bond.

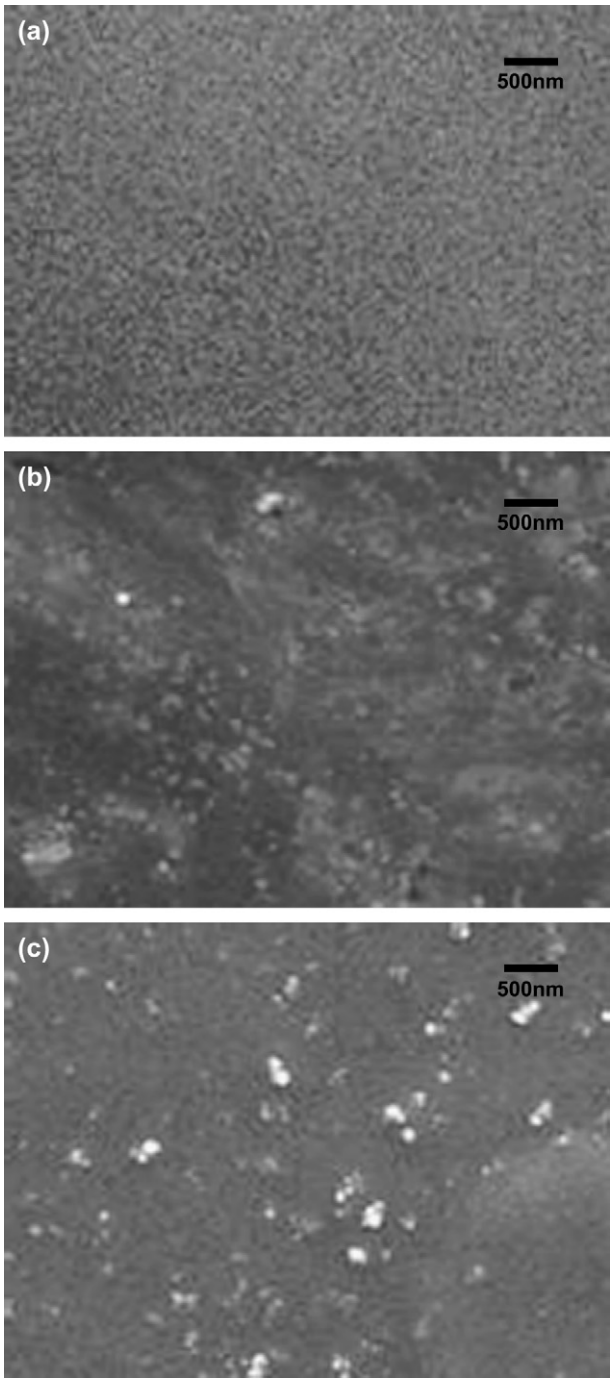

Fig. 8. SEM images of PHB-HHx/hydrophobically modified silica hybrid composites (scale bar: 500 nm): (a) PHB-HHx, (b) PHB-HHx/Si (1 wt%), and (c) PHB-HHx/Si (5 wt%).

maximum crystallization temperature shifts to a lower temperature for all samples. Generally, when a specimen is cooled quickly, a greater degree of supercooling is required to initiate the crystallization, presumably as the motion of the PHB-HHx molecule is unable to follow the cooling rate. On the other hand, for a given cooling rate, with the increase of silica content, the crystallization temperature of the hybrid composites shifts to a lower temperature with a gradual widening in the range.

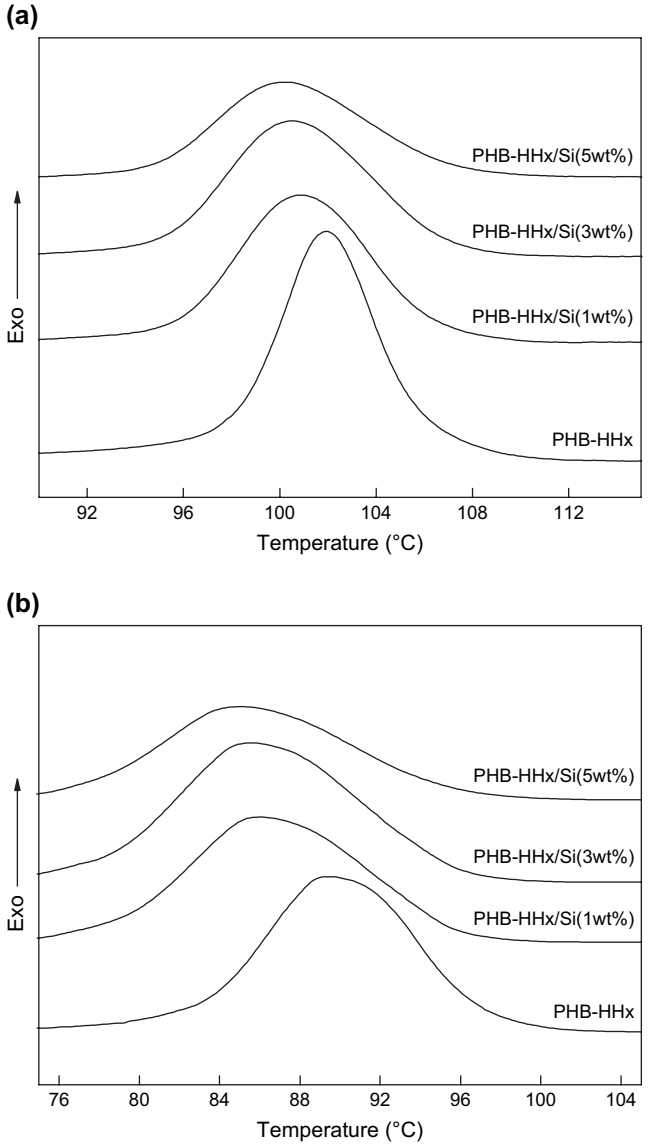

Fig. 9. DSC cooling curves of PHB-HHx/hydrophobically modified silica hybrids: (a) 1 °C min^{-1} cooling rate and (b) 3 °C min^{-1} cooling rate.

By using the observed T_c values, the fastest crystallization time (t_{max}) for various cooling rates was determined. The results are shown in Fig. 10, where t_{max} is defined as the time from the onset of crystallization to the appearance of the crystallization peak temperature. t_{max} can be expressed as a function of temperature (T) and the cooling rate (R) as [17]:

$$t_{max} = \frac{T_0 - T_c}{R} \quad (1)$$

where T_0 is the onset temperature of crystallization. For a given cooling rate, the t_{max} of the hybrid composites increases with the silica content, a result consistent with the intensity of the intermolecular hydrogen bonding between PHB-HHx and silica. Kuo et al. investigated the effect of hydrogen bond strength on the crystallization behavior of PCL blends, and they concluded that the crystallization rates of blends were reduced because of the strong intermolecular interaction

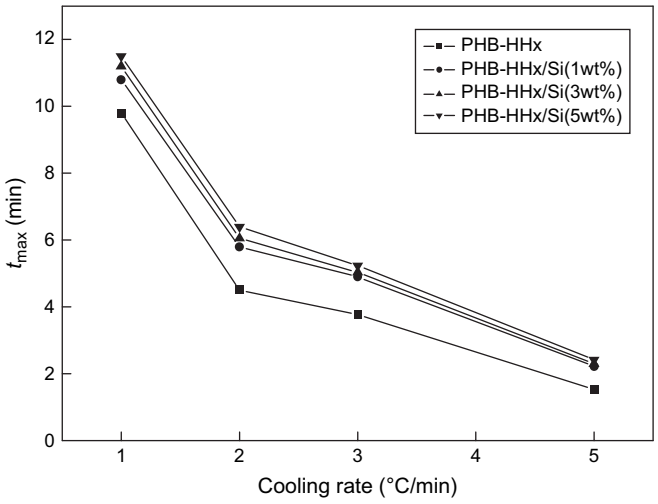

Fig. 10. The values of fastest crystallization time (t_{max}) for PHB-HHx/hydrophobically modified silica hybrids at various cooling rates.

between blend components [18]. On that basis, it could also be suggested that the addition of silica hinders the formation of PHB-HHx nuclei due to the existence of relatively strong intermolecular hydrogen bonding, thereby requiring more time to produce PHB-HHx crystals.

Crystallization rate coefficient (CRC) may be used to characterize the non-isothermal crystallization rate of the PHB-HHx/hydrophobically modified silica hybrid composites in detail [19,20]. CRC can be defined as:

$$\mathrm{CRC} = \frac{\Delta R}{\Delta T_c} \tag{2}$$

where R is the cooling rate and T_c is the crystallization temperature. It can be calculated from the slope of a plot of cooling rate *vs.* crystallization temperature. The larger the slope is, the faster the crystallization rate is. Fig. 11 shows the cooling rate *vs.* crystallization temperature for the PHB-HHx/hydrophobically modified silica hybrid composites, where the slope of the regression line can be used to determine the CRC of the hybrid composites ($R^2 = 0.975$). As seen in the Fig. 11, the slopes of the PHB-HHx/silica hybrids decreased as the silica content increased. Fig. 12 shows the variation in CRC as a function of the intermolecular hydrogen bond fraction in the PHB-HHx/hydrophobically modified silica hybrid composites and demonstrates that CRC gradually decreases as the extent of intermolecular hydrogen bonding increases. Clearly, intermolecular hydrogen bonding between the PHB-HHx and silica inhibits the mobility of the PHB-HHx chains and causes the non-isothermal crystallization rate of the PHB-HHx/silica hybrids to slow down. The relationship between the extent of intermolecular hydrogen bonding and CRC can be fitted by an empirical second-order equation ($Y = 13.1 - 0.28X + 0.009X^2$). This result may be explained such that, as the silica content increases, the increasing ratio of intermolecular hydrogen bonding becomes relatively lower as already seen in the FT-IR results. Thus the relationship between the extent of intermolecular hydrogen bonding and the non-crystallization rate cannot be described by a simple linear equation.

3.4. Isothermal crystallization kinetics

Fig. 13 exhibits the development of relative crystallinity with time for the PHB-HHx/hydrophobically modified silica hybrid composites at the isothermal crystallization temperature of 70 °C, where the relative crystallinity, X_t, was obtained from the ratio of the area of the exotherm up to time t, divided by the total isothermal crystallization exotherm. All isotherms exhibit a sigmoidal dependence on time. On the whole, the isotherms shift gradually toward longer crystallization times with increasing silica content. The induction time also increases with the silica content, proving that the isothermal crystallization rate becomes slower with increasing silica content in the hybrid composites.

Fig. 14(a)–(c) shows the spherulitic morphology of pure PHB-HHx and PHB-HHx/hydrophobically modified silica

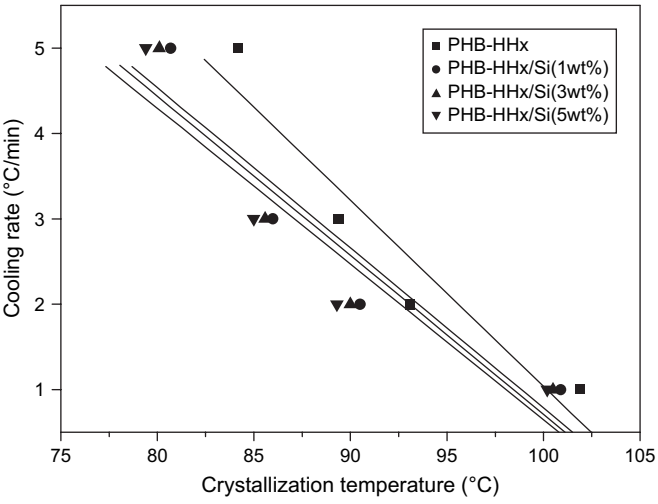

Fig. 11. Cooling rate *vs.* crystallization temperature for the PHB-HHx/hydrophobically modified silica hybrid composites.

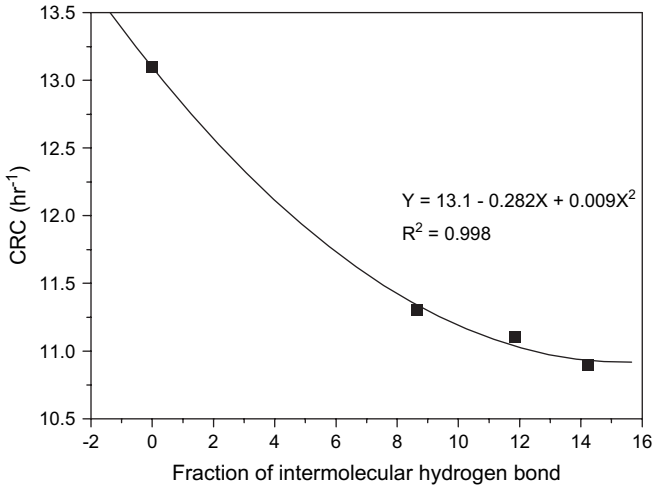

Fig. 12. The variation of CRC as a function of the intermolecular hydrogen bond fraction in PHB-HHx/hydrophobically modified silica hybrid composites.

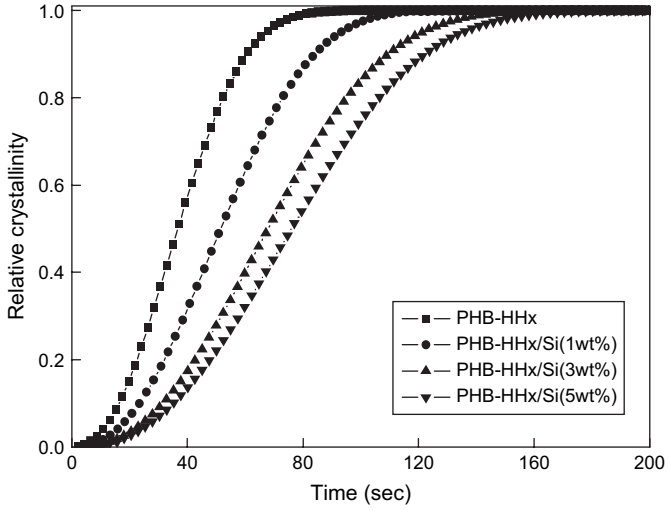

Fig. 13. The relative crystallinity *vs.* time at the 70 °C isothermal crystallization temperature for PHB-HHx/hydrophobically modified silica hybrid composites.

hybrid composites crystallized at 70 °C after melting. The pure PHB-HHx spherulites show the familiar Maltese cross birefringent pattern and concentric extinction bands. For the hybrid composites, the band spacing increases with the silica content. Generally, the banded structure of spherulites is believed to be due to the presence of twisted lamellae resulting from stress build up during crystallization and it probably occurs within disordered fold surfaces of the polymer crystal [21,22]. It has been reported that the band spacing usually increases as the crystal growth rate decreases and the crystallization temperature increases [23]. Consequently, this result strongly supports the hypothesis that silica reduces the isothermal crystallization rate of the PHB-HHx in their hybrids.

The isothermal crystallization rates of the PHB-HHx/hydrophobically modified silica hybrid composites were investigated in detail by measuring the half-time of crystallization, $t_{1/2}$. Their values are listed in Table 2. For a given crystallization temperature, the $t_{1/2}$ for a hybrid composite is slower than that of pure PHB-HHx. It also becomes slower with the increase of silica content. Hence, as the silica content increases, the segmental mobility of the PHB-HHx molecules is restricted due to a much greater degree of intermolecular hydrogen bonding, which results in slowing down of the isothermal crystallization rates in the hybrid composites.

Fig. 15 shows the Avrami plot of PHB-HHx/hydrophobically modified silica hybrid composites at $T_c = 70$ °C. The Avrami equation is defined as [24,25]:

$$\log[-\ln(1-X_t)] = \log K + n \log t \tag{3}$$

the Avrami exponent, n, is correlated to the nucleation mechanism and geometry of crystal growth. The overall crystallization rate, $\tau_{0.5}$, is defined as the reciprocal of the half-time of crystallization and it is commonly used to describe the overall crystallization rate. The values of the rate parameters n and

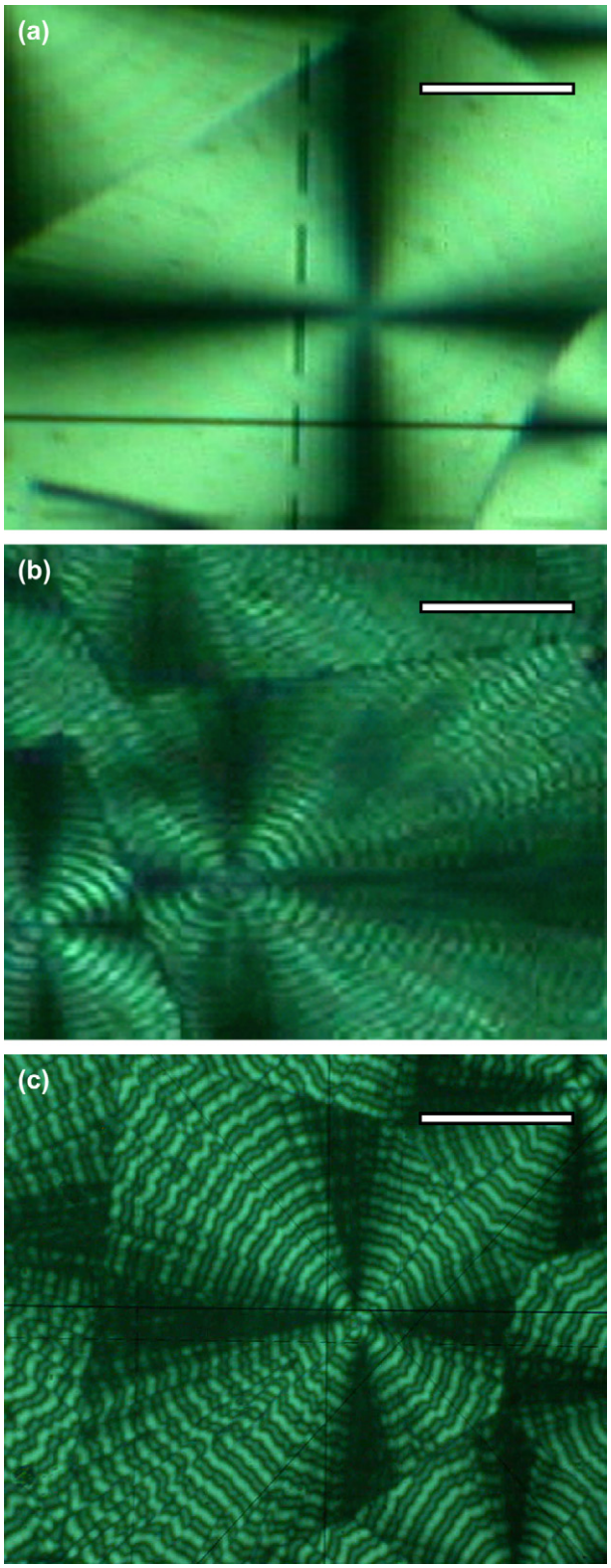

Fig. 14. Spherulitic morphology of PHB-HHx/hydrophobically modified silica hybrid composites crystallized at 70 °C (scale bar: 25 μm): (a) PHB-HHx, (b) PHB-HHx/Si (1 wt%), and (c) PHB-HHx/Si (5 wt%).

$\tau_{0.5}$ obtained from the Avrami equation are listed in Table 2. Regardless of the silica content and isothermal crystallization temperature, n is essentially constant. This result indicates

Table 2
The rate parameters obtained from the Avrami equation for the PHB-HHx/hydrophobically modified silica hybrid composites

Sample	65 °C			70 °C			75 °C			85 °C		
	n	$t_{1/2}$ (s)	$\tau_{0.5} \times 10^3$ (s^{-1})	n	$t_{1/2}$ (s)	$\tau_{0.5} \times 10^3$ (s^{-1})	n	$t_{1/2}$ (s)	$\tau_{0.5} \times 10^3$ (s^{-1})	n	$t_{1/2}$ (s)	$\tau_{0.5} \times 10^3$ (s^{-1})
PHB-HHx	2.3	39.1	25.6	2.3	36.7	27.2	2.4	57.2	17.5	2.5	82.7	12.1
PHB-HHx/Si (1 wt%)	2.4	58.2	17.2	2.4	51.8	19.3	2.5	58.3	17.2	2.6	87.7	11.4
PHB-HHx/Si (3 wt%)	2.4	86.6	11.5	2.5	68	14.7	2.5	94.5	10.6	2.4	101.9	9.8
PHB-HHx/Si (5 wt%)	2.5	87.4	11.4	2.5	76.1	13.1	2.4	102.8	9.7	2.5	127.6	7.8

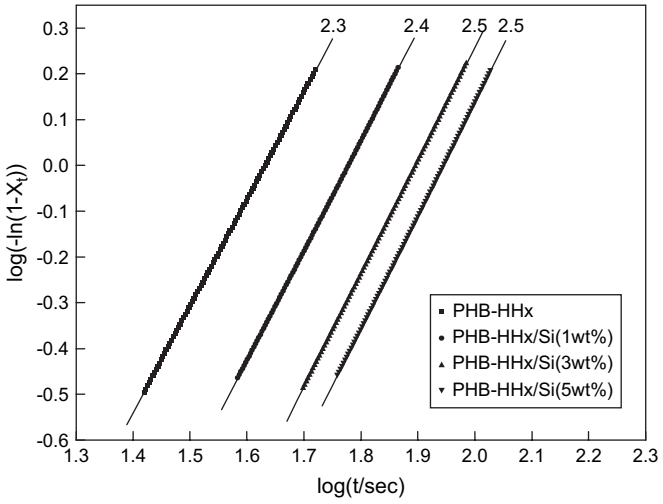

Fig. 15. The Avrami plot of PHB-HHx/hydrophobically modified silica hybrid composites at $T_c = 70$ °C.

that the silica has little effect on either the nucleation mechanism or the geometry of crystal growth of the PHB-HHx in their hybrid composites. On the other hand, for a given crystallization temperature, the $\tau_{0.5}$ value of the PHB-HHx/hydrophobically modified silica hybrids decreases gradually as the silica content increases, supporting the notion that the overall crystallization rates of the PHB-HHx/hydrophobically modified silica hybrids are retarded by the addition of silica.

The crystallization activation energy, ΔE, was determined by using the Arrhenius equation for the PHB-HHx/hydrophobically modified silica hybrid composites [26]. Fig. 16 shows the plots of $(1/n)\ln K$ *vs.* $1/T_c$ for the PHB-HHx/silica hybrid composites. The slope of the regression line in Fig. 16 can be used to determine the ΔE of the hybrid composites. The ΔE of neat PHB-HHx was -48.6 kJ mol^{-1}. It can be seen that the higher the silica content is, the larger the absolute value of ΔE is for the PHB-HHx/hydrophobically modified silica hybrid composites. For the PHB-HHx/silica (5 wt%) hybrids, ΔE was -54.5 kJ mol^{-1}. Fig. 17 shows the correlation of absolute activation energy as a function of the intermolecular hydrogen bond fraction in the PHB-HHx/hydrophobically modified silica hybrid composites. The greater the extent of intermolecular hydrogen bonding is, the higher the activation energy, confirming that more activation energy is required for crystallization in the PHB-HHx/silica hybrid composites, most likely because the intermolecular hydrogen bonding between the PHB-HHx and silica retards the overall crystallization rate of PHB-HHx in their hybrid composites. In other words, their variation also corresponds to the empirical second-order equation: $Y = 48.6 + 0.70X - 0.02X^2$, found for the non-isothermal crystallization rates. Furthermore, the validity of this fit is very high, where reliability is 0.9992. This result again supports the point that the relationship between

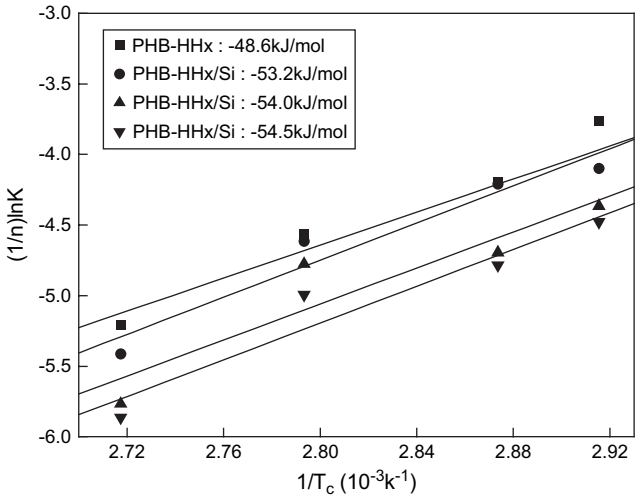

Fig. 16. Plots of $(1/n)\ln K$ *vs.* $1/T_c$ for PHB-HHx/hydrophobically modified silica hybrid composites.

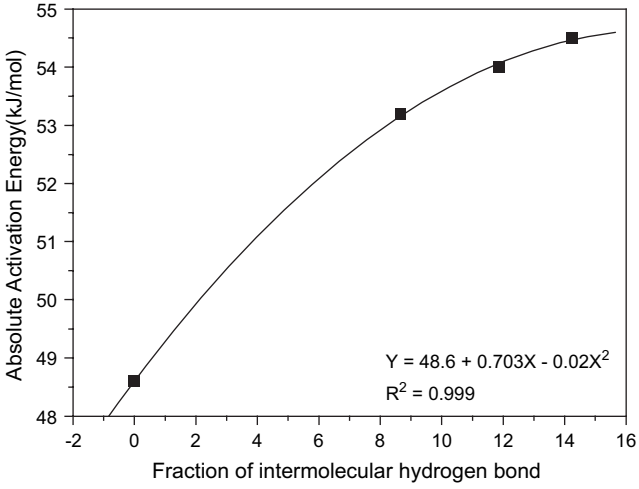

Fig. 17. The absolute activation energy as a function of the intermolecular hydrogen bond fraction in PHB-HHx/hydrophobically modified silica hybrid composites.

the extent of intermolecular hydrogen bonding and the crystallization rate cannot have a linear equation, since the added silica content is not directly proportional to the extent of intermolecular hydrogen bonding.

4. Conclusions

A series of biodegradable PHB-HHx/silica hybrid composites were prepared by using simple melt compounding and used to investigate the effect of hydrogen bonding on the crystallization behavior of the composites. Compared with PHB-HHx/hydrophilic silica hybrids, the PHB-HHx/hydrophobically silica hybrids had stronger intermolecular hydrogen bonds. As the silica content increased, the intermolecular hydrogen bonding between the PHB-HHx and hydrophobically modified silica was stronger. However, the extent of intermolecular hydrogen bonding was not directly proportional to the amount of added silica. The silica reduced the non-isothermal and isothermal crystallization rates of PHB-HHx in the hybrids, and these were ordered by the strength of intermolecular hydrogen bonding between the PHB-HHx and silica. The constant value of the Avrami exponent demonstrated that the presence of silica did not change the nucleation mechanism or the geometry of crystal growth from PHB-HHx in their hybrid composites. The values obtained for the crystallization activation energy supported that the silica retarded the overall crystallization rate of PHB-HHx as a result of the formation of intermolecular hydrogen bonds between the PHB-HHx and silica in the hybrid composites. Finally, it was observed that the relationship between the extent of intermolecular hydrogen bond and crystallization rate was described by the empirical second-order equation.

Acknowledgment

This work was supported by the research fund of the Ministry of Commerce, Industry and Energy in Korea (Grant No. 2006-000-0000-2897).

References

[1] Tian D, Dubois PH, Jerome R. Polymer 1996;37:3983.
[2] Tian D, Dubois PH, Blacher S, Jerome R. Polymer 1997;39:855.
[3] Sinha Ray S, Maiti P, Okamoto M, Yamata K, Ueda K. Macromolecules 2002;35:3104.
[4] Wang YW, Wu Q, Chen J, Chen GQ. Biomaterials 2005;26:899.
[5] Wang YW, Wu Q, Chen GQ. Biomaterials 2003;24:4621.
[6] Chung SC, Hahm WG, Im SS, Oh SG. Macromol Res 2002;10:221.
[7] Technical bulletin no. 11, vol. 6. Akron, OH: Degussa Corporation; 1989.
[8] Kontou E, Niaounakis M. Polymer 2006;47:1267.
[9] Chan CK, Chu IM. Polymer 2001;42:6089.
[10] Vahik K, Darrin JP. Macromolecules 2004;37:6480.
[11] Nie K, Zheng S, Lu F, Zhu Q. J Polym Sci Part B Polym Phys 2005;43:2594.
[12] Lim JS, Noda I, Im SS. J Polym Sci Part B Polym Phys 2006;44:2852.
[13] Sato H, Murakami R, Padermshoke A, Hirose F, Senda K, Noda I, et al. Macromolecules 2004;37:7203.
[14] Viswanathan S, Dadmun MD. Macromolecules 2002;35:5049.
[15] Li D, Brisson J. Polymer 1998;39:793.
[16] Barthel H, Heinemann M, Stintz M, Wessely B. Part Part Syst Charact 1999;16:169.
[17] Kong X, Yang X, Li G, Zaho X, Zhou E, Ma D. Eur Polym J 2001;37:1855.
[18] Kuo SW, Chan SC, Chang FC. Macromolecules 2003;36:6653.
[19] Zhehui L, Philippe M, Robert J. Polymer 1997;38:5149.
[20] Khanna TP. Polym Eng Sci 1990;30:1615.
[21] Keith HD, Padden FJ. Polymer 1984;25:28.
[22] Fei B, Chen C, Wu H, Peng S, Wang X, Dong L, et al. Polymer 2004;45:6275.
[23] Penning JP, Manley SJ. Macromolecules 1996;29:84.
[24] Avrami M. J Chem Phys 1941;9:177.
[25] Avrami M. J Chem Phys 1939;7:1193.
[26] Cebe P, Hong SD. Polymer 1986;27:183.